OPEN ACCESS

TRANSLATIONAL SCIENCE

Long non-coding RNA HOTAIR drives EZH2-dependent myofibroblast activation in systemic sclerosis through miRNA 34a-dependent activation of NOTCH

Christopher W Wasson,[1] Giuseppina Abignano,[1,2,3] Heidi Hermes,[4] Maya Malaab,[5] Rebecca L Ross,[1] Sergio A Jimenez ,[4] Howard Y Chang,[6] Carol A Feghali-Bostwick,[5] Francesco del Galdo [1,3]

Handling editor Josef S Smolen

► Additional material is published online only. To view please visit the journal online (http://dx.doi.org/10.1136/annrheumdis-2019-216542).

For numbered affiliations see end of article.

Correspondence to
Professor Francesco del Galdo, Leeds Institute of Rheumatic and Musculoskeletal Medicine, University of Leeds, Leeds LS2 9JT, UK; f.delgaldo@leeds.ac.uk

GA and HH contributed equally.

Received 28 October 2019
Revised 8 January 2020
Accepted 9 January 2020
Published Online First
10 February 2020

To cite: Wasson CW, Abignano G, Hermes H, *et al*. *Ann Rheum Dis* 2020;**79**:507–517.

ABSTRACT

Background Systemic sclerosis (SSc) is characterised by autoimmune activation, tissue and vascular fibrosis in the skin and internal organs. Tissue fibrosis is driven by myofibroblasts, that are known to maintain their phenotype in vitro, which is associated with epigenetically driven trimethylation of lysine 27 of histone 3 (H3K27me3).

Methods Full-thickness skin biopsies were surgically obtained from the forearms of 12 adult patients with SSc of recent onset. Fibroblasts were isolated and cultured in monolayers and protein and RNA extracted. HOX transcript antisense RNA (HOTAIR) was expressed in healthy dermal fibroblasts by lentiviral induction employing a vector containing the specific sequence. Gamma secretase inhibitors were employed to block Notch signalling. Enhancer of zeste 2 (EZH2) was blocked with GSK126 inhibitor.

Results SSc myofibroblasts in vitro and SSc skin biopsies in vivo display high levels of HOTAIR, a scaffold long non-coding RNA known to direct the histone methyltransferase EZH2 to induce H3K27me3 in specific target genes. Overexpression of HOTAIR in dermal fibroblasts induced EZH2-dependent increase in collagen and α-SMA expression in vitro, as well as repression of miRNA-34A expression and consequent NOTCH pathway activation. Consistent with these findings, we show that SSc dermal fibroblast display decreased levels of miRNA-34a in vitro. Further, EZH2 inhibition rescued miRNA-34a levels and mitigated the profibrotic phenotype of both SSc and HOTAIR overexpressing fibroblasts in vitro.

Conclusions Our data indicate that the EZH2-dependent epigenetic phenotype of myofibroblasts is driven by HOTAIR and is linked to miRNA-34a repression-dependent activation of NOTCH signalling.

Key messages

What is already known about this subject?

- Enhancer of zeste 2 (EZH2) contributes to the epigenetically stable activation of dermal fibroblasts in systemic sclerosis (SSc).

What does this study add?

- Long non-coding RNA HOX transcript antisense RNA (HOTAIR) drives the specific methylation profile of EZH2 in SSc fibroblasts.
- The HOTAIR/EZH2-dependent profibrotic activation of SSc fibroblasts is mediated by NOTCH through miRNA-34a repression.

How might this impact on clinical practice or future developments?

- This study provides further details into the epigentic stable activation of SSc dermal fibroblasts which will help us understand how to target this pathway therapeutically.

INTRODUCTION

Systemic sclerosis (SSc) is a prototypic fibrotic disease that causes tissue and vascular fibrosis in the skin and internal organs including heart, lungs, kidneys and gastrointestinal tract.[1 2] Tissue fibrosis typically starts in the skin at the level of hands and feet[3] and progresses through the arms and thighs to eventually involve the chest and abdomen in the most severe cases (diffuse cutaneous SSc).[1]

Fibroblasts are the key cellular elements of fibrosis and once explanted from affected tissues they maintain their profibrotic phenotype in vitro, showing increased secretion of collagen and extracellular matrix proteins and higher frequency of alpha-smooth muscle actin (α-SMA) positive cells (myofibroblasts).[4 5] This epigenetic feature has allowed in-vitro studies which have detailed the molecular mechanisms linked to fibrosis including a key role for growth factors like transforming growth factor beta (TGF-β),[6–8] platelet-derived growth factor (PDGF)[9 10] and Notch signalling.[11 12]

The Notch family of cell surface receptors is important for cell-to-cell communication.[13] On ligand binding, the receptor is cleaved by gamma secretase proteases to release the intracellular domain Notch Intracellular Domain (NID),[14] which induces transcription of downstream targets.[15] NOTCH expression is known to be regulated by miRNAs such as miRNA-34a, which function as a suppressor of NOTCH expression.[16 17]

Recently, Tsou *et al*[18] have shown that enhancer of zeste 2 (EZH2) plays an important role in the epigenetic features linked to tissue fibrosis in SSc.

EZH2 is the enzymatic subunit of the polycomb repressor complex (PRC) that induces methylation of histone 3, therefore silencing target genes. Nevertheless, the signal directing the PRC to specific DNA regions responsible for the phenotype was not elucidated.

Scaffold lncRNAs are RNAs of at least 200 nucleotides with a 'W'-shaped tertiary structure.[19] This allows one domain to recognise specific DNA sequences and the other to bind the PRC, effectively focusing PRC activity in specific promoter regions.[20 21] There is increasing evidence that lncRNA plays an important role in a number of fibrotic conditions including liver,[22] myocardial[23] and renal fibrosis.[24] Particularly, lncRNAs within the HOX loci have been described as master epigenetic regulators within the connective tissue.[25] HOX transcript antisense RNA (HOTAIR) is one of the better characterised lncRNAs within the HOX locus. It has been shown to cooperate with PRC2 in mediating the EZH2-driven repression of homeobox D cluster through the spread of H3K27me3 methylation marker associated with gene silencing.[26–28]

Here, starting from the observation of increased HOTAIR expression in SSc fibroblasts cultured and SSc skin biopsies, we demonstrate that HOTAIR expression is sufficient to induce profibrotic activation of dermal fibroblasts in vitro. Further, we show that this phenotype is driven by NOTCH pathway activation which is mediated by EZH2-dependent repression of miRNA-34a expression.

METHODS

Detailed description of experimental methods is available as online supplementary file 1.

RESULTS

α-SMA positive fibroblasts show increased expression of HOTAIR in vitro and in vivo

Fibroblasts from SSc maintain in vitro their profibrotic phenotype, including increased α-SMA expression, indicating an epigenetically driven activation of these cells.[29 30] Immunofluorescence studies of SSc dermal fibroblasts and healthy control (HC) fibroblasts showed that the increased expression of α-SMA was due to increased number of α-SMA positive cells, rather than homogenous increase of α-SMA expression in all cells (figure 1A). lncRNA from the HOX locus are master regulators of the connective tissue. To investigate the role of this specific group of lncRNAs in the myofibroblast phenotype in SSc, we performed HOX tiling array as described by Rinn *et al*[25] on the RNA extracted from laser capture microdissected α-SMA positive or negative cells from dermal fibroblasts cultured from four SSc skin biopsies (figure 1B). Effectiveness of laser capture microdissection (figure 1B) was validated by quantitative real time (qRT)-PCR showing 3.5-fold increased mRNA levels for α-SMA (figure 1C). HOX tiling array on the extracted RNA showed a number of lncRNA from the HOX locus were upregulated (figure 1D). Interestingly, HOTAIR levels were elevated 2.05-fold in α-SMA-positive fibroblasts. HOTAIR is a known regulator of EZH2[27] and it is highly expressed in the hands and feet of humans.[25] Therefore, it was an interesting target for SSc. We validated the tiling array data by qPCR and observed a 2-fold increased levels of HOTAIR in α-SMA positive cells compared with α-SMA negative cells (figure 1E). SSc dermal fibroblasts (n=6) showed in vitro a 7-fold increase in HOTAIR levels compared with HC dermal fibroblasts (figure 1F). Clinical features and relative HOTAIR levels for each patient fibroblast cell line is found in online supplementary table 1.

To validate this finding in vivo, we analysed SSc skin biopsies for HOTAIR transcript levels both by qRT-PCR and in-situ hybridisation. SSc skin biopsies showed >100-fold increased expression of HOTAIR compared with HC skin (n=4) (figure 1G). Consistent with these findings, in-situ hybridisation of SSc skin biopsies showed increased localisation of HOTAIR in the dermis of SSc skin biopsies compared with HC (n=3) (figure 1H).

HOTAIR drives a profibrotic activation in dermal fibroblasts

To determine the role of HOTAIR in the profibrotic activation of dermal fibroblasts, we silenced HOTAIR expression in primary fibroblasts using long non-coding antisense (LNA) oligonucleotides for 72 hours. LNA efficiently reduced HOTAIR transcript levels (figure 1I). Silencing HOTAIR also resulted in a significant reduction in α-SMA and connective tissue growth factor (CTGF) transcript levels.

In a complementary approach, we set out to induce stable overexpression of HOTAIR (or scrambled RNA) in human dermal fibroblasts immortalised through retroviral induced expression of HTERT as previously described.[10] Immortalised dermal fibroblasts were infected with lentiviral particles carrying HOTAIR gene in frame with GFP and puromycin-resistance genes. Infected cells were visualised and positively sorted by green fluorescent protein(GFP) (figure 2A,B), to select the cells with highly efficient lentiviral integration, and maintained in media containing puromycin. qRT-PCR analysis for HOTAIR confirmed its increased expression in transduced cells compared with cells infected with lentivirus carrying a scrambled RNA sequence (figure 2C). We screened the scrambled and HOTAIR-expressing fibroblasts for profibrotic markers expression. Overexpression of HOTAIR in fibroblasts resulted in increased levels of collagen type 1A1, 1A2, α-SMA and CTGF transcript levels (figure 2D–G) . This was consistent with increased protein levels of collagen type 1 (3-fold) and α-SMA (2-fold), (figure 2H,I). Accordingly, HOTAIR-expressing fibroblasts showed pronounced expression of α-SMA fibres by immunofluorescence compared with scramble control fibroblasts (figure 2J). These data suggest that HOTAIR expression can induce expression of myofibroblast markers in vitro. Further, we observed that treatment with TGF-β treatment induced a 14-fold increase in α-SMA levels compared with untreated HOTAIR-expressing fibroblasts, which was 2-fold higher than the upregulation observed in scramble fibroblasts treated with TGF-β (figure 2K). This suggests that the overexpression of HOTAIR primes the fibroblasts for TGF-β mediated activation.

HOTAIR induces EZH2-dependent increase of H3K27me3 methylation marker

HOTAIR has been shown to cooperate with PRC2 to induce methylation of target gene promoter.[31 32] One member of the complex is the enzyme EZH2, which is essential for histone 3 trimethylation. Tsou *et al* have shown that EZH2 levels are increased in SSc fibroblasts and inhibition of EZH2 suppresses their profibrotic phenotype.[18] Here, we set out to determine whether HOTAIR overexpression enhances expression of EZH2 and methylation of histone 3 in dermal fibroblasts.

HOTAIR-expressing fibroblasts showed no significant difference in EZH2 transcript when compared with scrambled controls (figure 3A). On the contrary, levels of H3K27me3 were increased by 8-fold in HOTAIR-expressing fibroblasts, consistent with the role of HOTAIR in targeting EZH2 to specific DNA regions rather than increasing its expression (figure 3B,C).

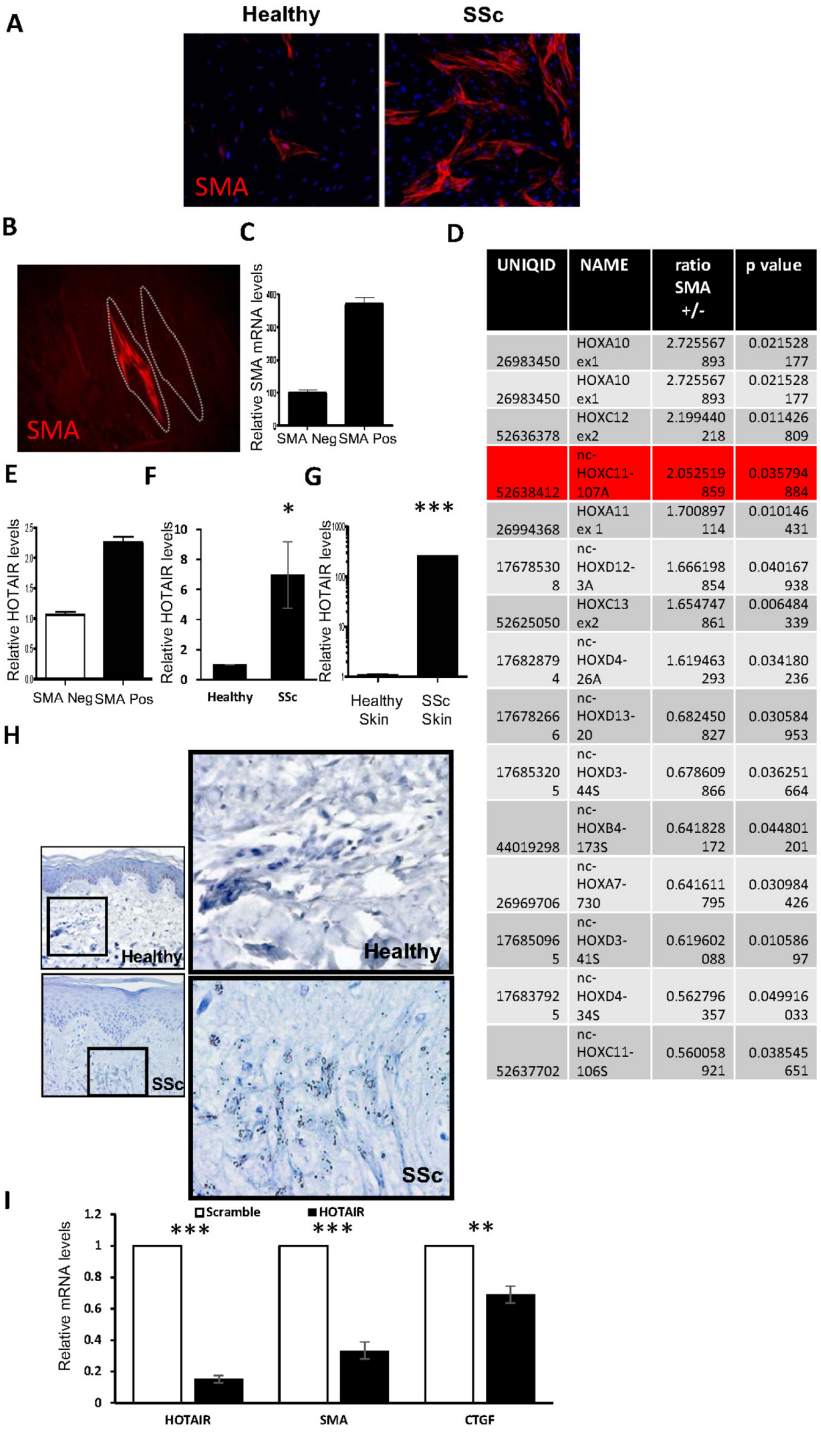

UNIQID	NAME	ratio SMA +/-	p value
26983450	HOXA10 ex1	2.725567893	0.021528177
26983450	HOXA10 ex1	2.725567893	0.021528177
52636378	HOXC12 ex2	2.199440218	0.011426809
52638412	nc-HOXC11-107A	2.052519859	0.035794884
26994368	HOXA11 ex 1	1.700897114	0.010146431
176785308	nc-HOXD12-3A	1.666198854	0.040167938
52625050	HOXC13 ex2	1.654747861	0.006484339
176828794	nc-HOXD4-26A	1.619463293	0.034180236
176782666	nc-HOXD13-20	0.682450827	0.030584953
176853205	nc-HOXD3-44S	0.678609866	0.036251664
44019298	nc-HOXB4-173S	0.641828172	0.044801201
26969706	nc-HOXA7-730	0.641611795	0.030984426
176850965	nc-HOXD3-41S	0.619602088	0.01058697
176837925	nc-HOXD4-34S	0.562796357	0.049916033
52637702	nc-HOXC11-106S	0.560058921	0.038545651

Figure 1 lncRNA HOX transcript antisense RNA (HOTAIR) is upregulated in activated myofibroblasts. (A) Healthy and systemic sclerosis (SSc) fibroblasts were stained with a mouse alpha-smooth muscle actin (α-SMA) antibody and visualised with an alexa 594-conjugated mouse secondary antibody (red). Cells were counterstained with 4′,6-diamidino-2-phenylindole (DAPI) to stain the nuclei (blue). (B) α-SMA positive or negative single cells were dissected by laser capture microscopy on untreated SSc patient fibroblasts. RNA was extracted from α-SMA positive and negative cells. (C) α-SMA transcript levels were assessed by qPCR. Graph represents mRNA levels from three independent repeats. (D) HOX tiling array was performed on the RNA and the table represents the fold differences of each lncRNA within the HOX locus in α-SMA positive cells compared with negative. HOTAIR is labelled in red. (E) HOTAIR transcript levels were assessed from RNA extracted from α-SMA positive and negative cells by qPCR. Graph represents mRNA levels from three independent repeats. (F) RNA was extracted from telomerase reverse transcriptase (Human) (HTERT) immortalised fibroblasts that had been isolated from healthy and patient with SSc skin biopsies. HOTAIR transcript levels were assessed by qPCR. Graph represents HOTAIR mRNA levels from five healthy patients and five patient with diffuse SSc fibroblasts. (G) RNA was extracted from healthy and patient with diffuse SSc skin biopsies. HOTAIR transcript levels were assessed by qPCR. Graph represents HOTAIR mRNA levels from (n=3). (H) HOTAIR in situ hybridisation staining from healthy and patient with SSc skin. (H) Expanded panels represent areas of interest in the dermis regions and black boxes represent the region of the area of interest. (I) RNA was extracted from primary fibroblasts transfected with HOTAIR and scramble control antisense oligonucleotides. HOTAIR, α-SMA and connective tissue growth factor (CTGF) transcript levels were assessed by qPCR. Graph represents mRNA levels from three independent repeats. *p<0.05, **p<0.01, ***p<0.001.

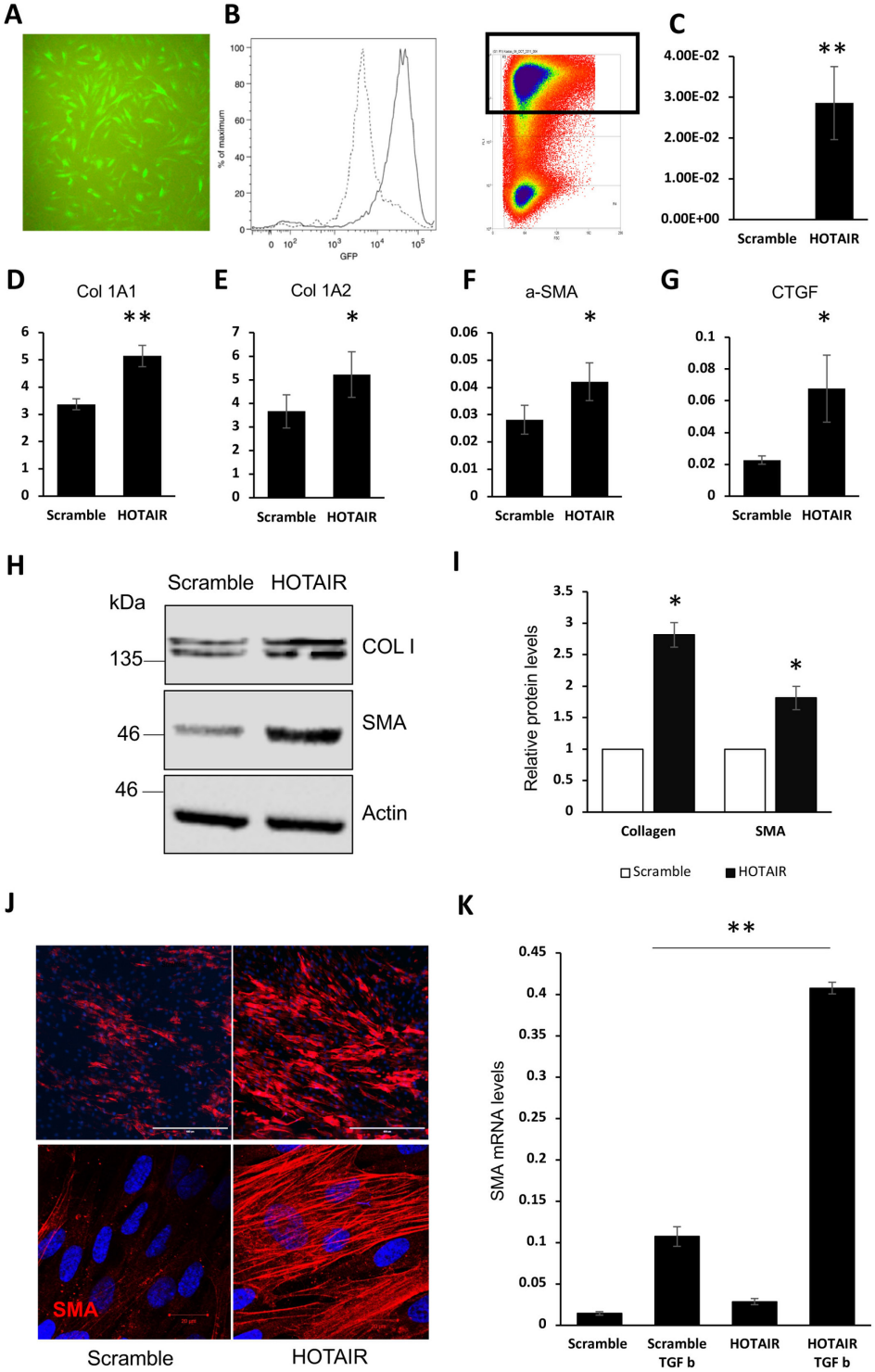

Figure 2 HOX transcript antisense RNA (HOTAIR) drives profibrotic activation of dermal fibroblasts. (A) Representative image of healthy dermal fibroblasts infected with lentiviruses containing the scramble/HOTAIR vectors. Vectors contain a GFP reporter to determine infection efficiencies. (B) Histograms representing GFP cell sorting of fibroblasts-infected lentiviruses containing the scramble/HOTAIR vectors. GFP-positive fibroblasts were collected and cultured. RNA was extracted from fibroblasts stably expressing scramble and HOTAIR vectors. (C) HOTAIR, (D) collagen type 1A1, (E) 1A2, (F) alpha-smooth muscle actin (α-SMA) and (G) connective tissue growth factor (CTGF) transcript levels were assessed by qPCR. Graphs represents mRNA levels from three independent repeats. (H) Protein was extracted from fibroblasts stably expressing scramble and HOTAIR vectors. Lysates were probed with a pan collagen type 1 antibody and an α-SMA antibody by western blot. β-actin was probed for as a loading control. (I) Graph represents densitometry analysis of collagen type 1 and α-SMA western blots from three independent repeats. (J) α-SMA staining of scramble and HOTAIR expressing dermal fibroblasts. Fibroblasts were stained with a mouse α-SMA antibody and visualised with a mouse-specific alexa 594-conjugated secondary (red). Cells were counterstained with DAPI to visualise nuclei (blue). White lines represent 400 µM scale bar. Red lines represent 20 µM scale bar. Scramble and HOTAIR expressing fibroblasts were serum depleted for 16 hours prior to stimulation with TGF-β (10 ng/mL) for 48 hours. (K) RNA was extracted and α-SMA transcript levels were assessed by qPCR. Graphs represents mRNA levels from three independent repeats. *p<0.05, **p<0.01, ***p<0.001.

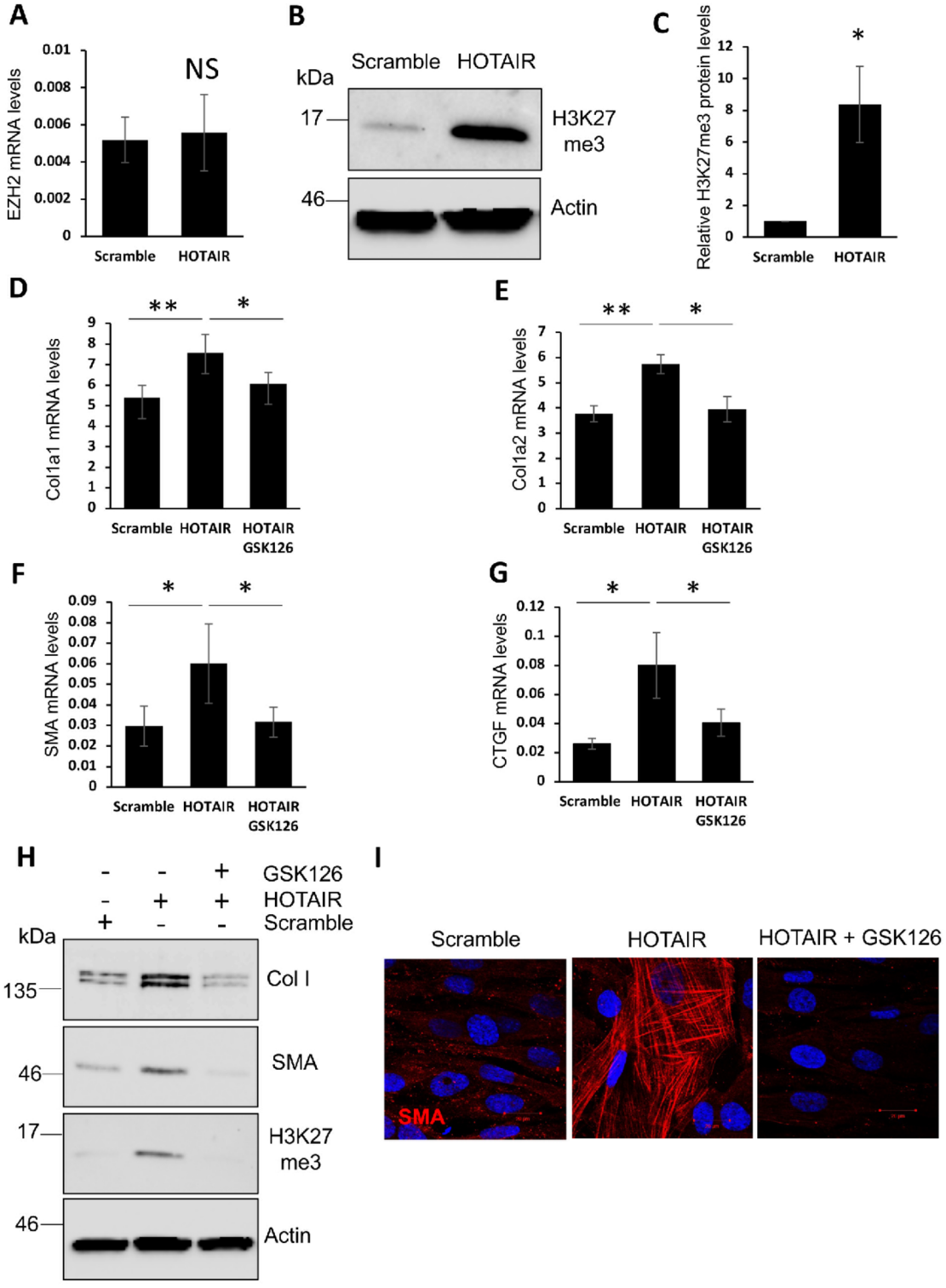

Figure 3 HOX transcript antisense RNA (HOTAIR) drives profibrotic activation through enhancer of zeste 2 (EZH2)-mediated H3K27me3 methylation. RNA was extracted from fibroblasts stably expressing scramble and HOTAIR vectors. (A) EZH2 transcript levels were assessed by qPCR. Graphs represents mRNA levels from three independent repeats. (B) Protein was extracted from fibroblasts stably expressing scramble and HOTAIR vectors. Lysates were probed with H3K27me3-specific antibody by western blot. β-actin was probed for as a loading control. (C) Graph represents densitometry analysis of H3K27me3 western blots from three independent repeats. RNA and protein were extracted from fibroblasts stably expressing the scramble and HOTAIR vectors, in addition to HOTAIR fibroblasts treated with the EZH2 inhibitor GSK126. (D) Collagen type 1A1, (E) collagen type 1A2, (F) alpha-smooth muscle actin (α-SMA) and (G) connective tissue growth factor (CTGF) transcript levels were assessed by qPCR. Graphs represents mRNA levels from three independent repeats. (H) Protein lysates were probed with pan collagen type 1, α-SMA and H3K27me3 antibodies by western blot. β-actin was probed for as a loading control. (I) α-SMA staining of scramble and HOTAIR expressing dermal fibroblasts in addition to HOTAIR fibroblasts treated with the EZH2 inhibitor GSK126. Fibroblasts were stained with a mouse α-SMA antibody and visualised with a mouse-specific alexa 594-conjugated secondary (red). Cells were counterstained with DAPI to visualise nuclei (blue). Red lines represent 20 µM scale bar. *p<0.05, **p<0.01, ***p<0.001. NS, not significant.

To determine whether HOTAIR induced profibrotic activation through EZH2, we employed the EZH2 inhibitor GSK126.[18 33] HOTAIR-expressing fibroblasts treated for 48 hours with GSK126 displayed reduced Col1A1, Col1A2, α-SMA and CTGF gene expression to levels comparable to scramble fibroblasts (figure 3D–G). This correlated with a reduction in collagen type 1 and α-SMA protein levels when HOTAIR-expressing fibroblasts were treated with the inhibitor (figure 3H,I). As expected, expression of H3K27me3 was lost on treatment with GSK126 (figure 3H). Importantly, inhibition of EZH2 with GSK126 also suppressed the increased collagen and α-SMA expression of SSc dermal fibroblasts (online supplementary figure 1) confirming the work of Tsou *et al*.[18]

HOTAIR primes myofibroblast differentiation through Notch activation

Notch signalling plays an important role in the fibrotic phenotype of SSc fibroblasts and in scleroderma animal models.[11 12 34] HOTAIR has previously been shown to enhance Notch expression and signalling in keratinocytes and retinoblastoma tissue.[35–37] In addition, EZH2 is known to play an important role in enhancing Notch1 transcription.[16 38] Therefore, we set out to determine whether HOTAIR expression could drive a EZH2-dependent increase in Notch expression in dermal fibroblasts and could Notch mediate the profibrotic effects of HOTAIR.

RNA levels of Notch1 were twofold higher in the HOTAIR-expressing fibroblasts compared with scramble control (figure 4A). NOTCH activation results in the cleavage of NID, which in turn is responsible for the target gene effects (figure 4B). Accordingly, HOTAIR-expressing fibroblasts showed increased levels of NID compared with the scramble control (figure 4C). In addition, levels of Hes1 (Notch responsive gene) were increased in the HOTAIR-expressing fibroblasts (figure 4D). These data supported the hypothesis that Notch signalling is increased in HOTAIR-expressing dermal fibroblasts.

To determine whether the increased NOTCH signalling observed in HOTAIR-expressing fibroblasts was EZH2 dependent, we looked at Notch1 transcript levels in HOTAIR-expressing fibroblasts treated with the GSK126 for 48 hours (figure 4E). Notch1 transcript levels were significantly reduced on GSK126 treatment. We also observed a reduction in NID levels in HOTAIR-expressing fibroblasts treated with GSK126 (figure 4F). Importantly, SSc fibroblasts showed increased Notch1 transcript levels compared with the healthy fibroblasts, consistent with published data (figure 4G).[11] The addition of the EZH2 inhibitor for 48 hours reduced Notch1 transcript. These data suggest that the ability of HOTAIR to regulate H3 trimethylation is important for Notch1 transcription.

To determine whether Notch signalling plays a role in HOTAIR-induced profibrotic fibroblast activation, we treated HOTAIR-expressing fibroblasts with the gamma secretase inhibitor RO4929097, which is known to block the gamma secretase responsible for cleaving the intracellular domain of NOTCH from the plasma membrane protein.[39] HOTAIR-expressing fibroblasts treated with RO4929097 showed a reduction in Hes1 transcript levels to levels comparable to Scrambled control (figure 4H). Most importantly, RO4929097 treated HOTAIR-expressing fibroblasts showed a reduction in collagen 1A1 and α-SMA expression to levels comparable to scrambled controls both at mRNA and protein levels (figure 4I–L).

We observed similar results with a second distinct gamma secretase inhibitor DAPT, a non-transition state analogue which blocks gamma secretase with a different mechanism of action[40] (online supplementary figure 2A). Following the same experimental approach, we treated HOTAIR-expressing fibroblasts with DAPT and assessed Col1A1 transcript levels. Like R04929097, DAPT reduced Col1A1 transcript levels in the HOTAIR-expressing fibroblasts to levels similar to the scramble control (online supplementary figure 2C). Hes1 transcript levels were also reduced confirming the inhibitor was active (online supplementary figure 2B). mRNA data were confirmed at protein level where we observed a reduction of the HOTAIR-expressing fibroblasts enhanced collagen type 1 and α-SMA protein levels in DAPT-treated cells to levels comparable to scramble controls (online supplementary figure 2D).

HOTAIR derepresses NOTCH1 expression through EZH2-dependent methylation of miRNA-34a

We next wanted to identify the mechanism HOTAIR employs to enhance Notch1 transcription. HOTAIR cannot target EZH2 directly to the Notch1 promoter because this would lead to suppression of Notch1 transcription. Therefore, HOTAIR must target a negative regulator of Notch1 transcription. Kwon *et al* have recently shown that EZH2 increases Notch1 transcription by methylation of miRNA-34a.[16] Hence, we determined miRNA-34a transcript levels in the scramble and HOTAIR-expressing fibroblasts. Expression of HOTAIR supressed miRNA-34a transcript levels in fibroblasts by 50%, which was completely reversed by EZH2 inhibition through GSK126 (figure 5B). We observed similar data in SSc fibroblasts. miRNA-34a transcript levels were reduced in SSc fibroblasts by 60% compared with healthy fibroblasts and this suppression of miRNA-34a was completely reverted on treatment with GSK126 to levels higher than HCs (figure 5C). These data indicate that the observed increased expression of Notch1 driven by HOTAIR in linked to repression of miRNA-34a. To determine the role of miRNA-34a suppression in the increased Notch1 expression of HOTAIR and SSc fibroblasts, we employed miRNA-34a mimics. Overexpression of miRNA-34a in HOTAIR-expressing fibroblasts reduced Notch1 transcript levels by 30% (figure 5D–E). In addition, overexpression of miRNA-34a supressed the levels of NID in HOTAIR expressing fibroblasts (figure 5F). Similar results were observed when miRNA-34a was overexpressed in SSc fibroblasts. Overexpression of miRNA-34a led to a 50% reduction in Notch1 transcript levels in the SSc fibroblasts (figure 5G,H). Accordingly, levels of NID and Hes1 were reduced in SSc fibroblasts were miRNA-34a was overexpressed (figure 5I–J). These data indicated that suppression of Notch1 transcription by overexpression of miRNA-34a in SSc fibroblasts was sufficient to supress Notch signalling. Taken together, these data show that HOTAIR enhances Notch1 expression and signalling through the suppression of miRNA-34a in an EZH2-dependent manner (figure 5A)

HOTAIR-mediated suppression of miRNA-34a is important for SSc fibrosis

We have shown that miRNA-34a suppressed Notch1 expression in both HOTAIR-expressing and SSc fibroblasts. We therefore wanted to investigate whether this led to a reduction in the profibrotic phenotype in both types of fibroblasts. Overexpression of miRNA-34a in HOTAIR-expressing fibroblasts reduced Col1a1, 1A2 and α-SMA transcript levels (figure 6A–C). This correlated with a reduction in collagen type 1 and α-SMA protein levels when HOTAIR-expressing fibroblasts were transfected with the miRNA-34a mimic (figure 6D,E). Similar results were observed in SSc fibroblasts when miRNA-34a was overexpressed.

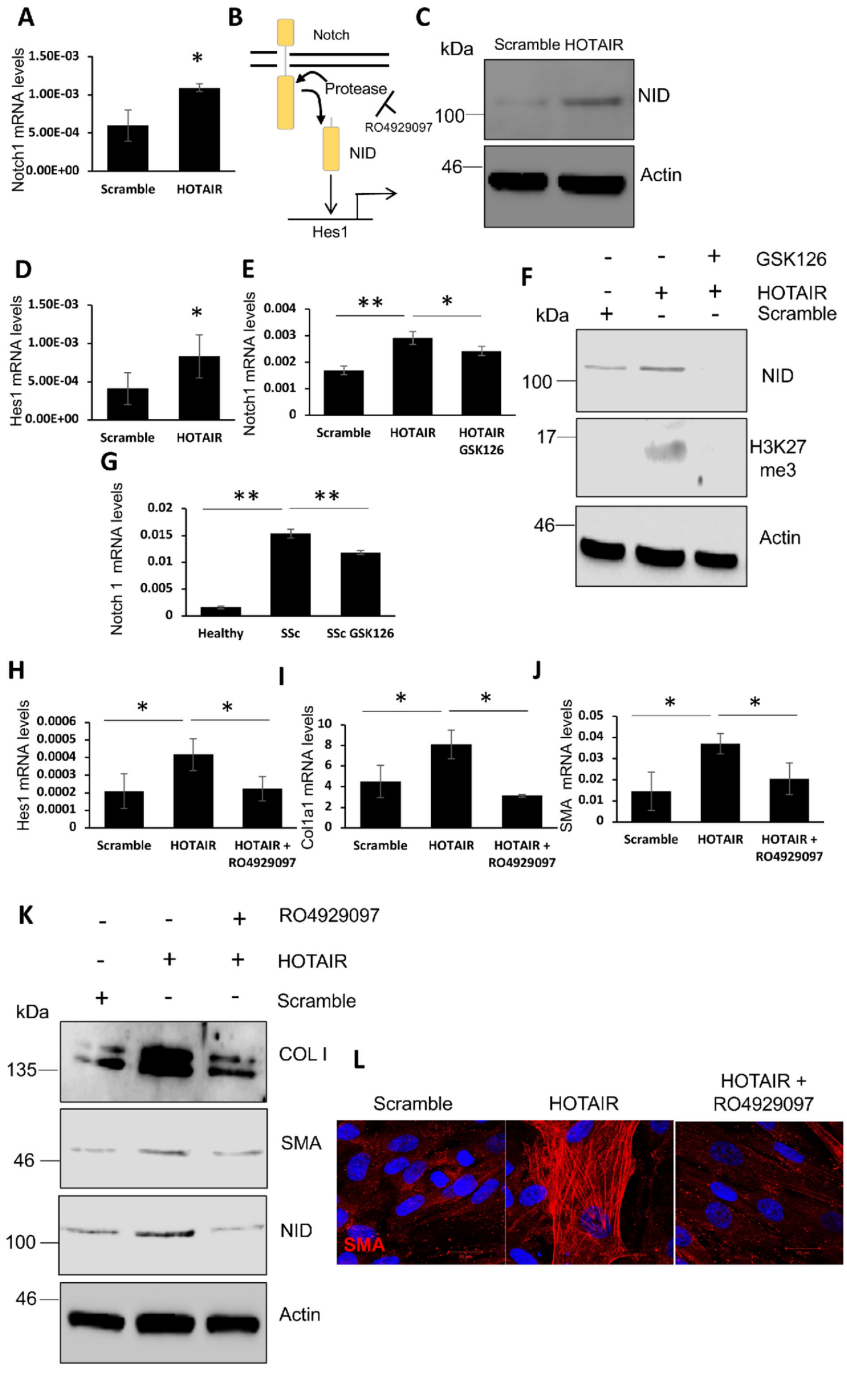

Figure 4 HOX transcript antisense RNA (HOTAIR) drives Notch 1 expression in dermal fibroblasts through enhancer of zeste 2 (EZH2). RNA was extracted from fibroblasts stably expressing scramble and HOTAIR vectors. (A) Notch1 and (D) Notch target gene Hes1 transcript levels were assessed by qPCR. Graph represents mRNA levels from three independent repeats. (B) Schematic of the Notch 1 receptor and the mechanism of activation. (C) Protein was extracted from fibroblasts stably expressing scramble and HOTAIR vectors. Lysates were probed with an antibody specific for the intracellular domain of Notch, Notch Intracellular Domain (NID) by western blot. β-actin was probed for as a loading control. (E) RNA and protein were extracted from fibroblasts stably expressing the scramble and HOTAIR vectors, in addition to HOTAIR fibroblasts treated with the EZH2 inhibitor GSK126. Notch 1 transcript levels were assessed by qPCR. Graphs represents mRNA levels from three independent repeats. (F) Protein lysates were probed with an NID and H3K27me3 antibodies by western blot. β-actin was probed for as a loading control. RNA was extracted from healthy and systemic sclerosis (SSc) fibroblasts, in addition to SSc fibroblasts treated with the EZH2 inhibitor GSK126. (G) Notch 1 transcript levels were assessed by qPCR. Graphs represents mRNA levels from three independent repeats. RNA and protein were extracted from fibroblasts stably expressing the scramble and HOTAIR vectors, in addition to HOTAIR fibroblasts treated with the gamma secretase inhibitor R04929097. (H) Hes1, (I) Col1A1 and (J) alpha-smooth muscle actin (α-SMA) transcript levels were assessed by qPCR. Graphs represents mRNA levels from three independent repeats. (K) Protein lysates were probed with a pan collagen type 1 antibody, an α-SMA antibody and an antibody specific for the intracellular domain of Notch 1 (NID) by western blot. β-actin was probed for as a loading control. (L) α-SMA staining of scramble and HOTAIR expressing dermal fibroblasts, in addition to HOTAIR fibroblasts treated with the gamma secretase inhibitor R04929097. Fibroblasts were stained with a mouse α-SMA antibody and visualised with a mouse-specific alexa 594-conjugated secondary (red). Cells were counterstained with DAPI to visualise nuclei (blue). Red lines represent 20 µM scale bar. *p<0.05, **p<0.01, ***p<0.001.

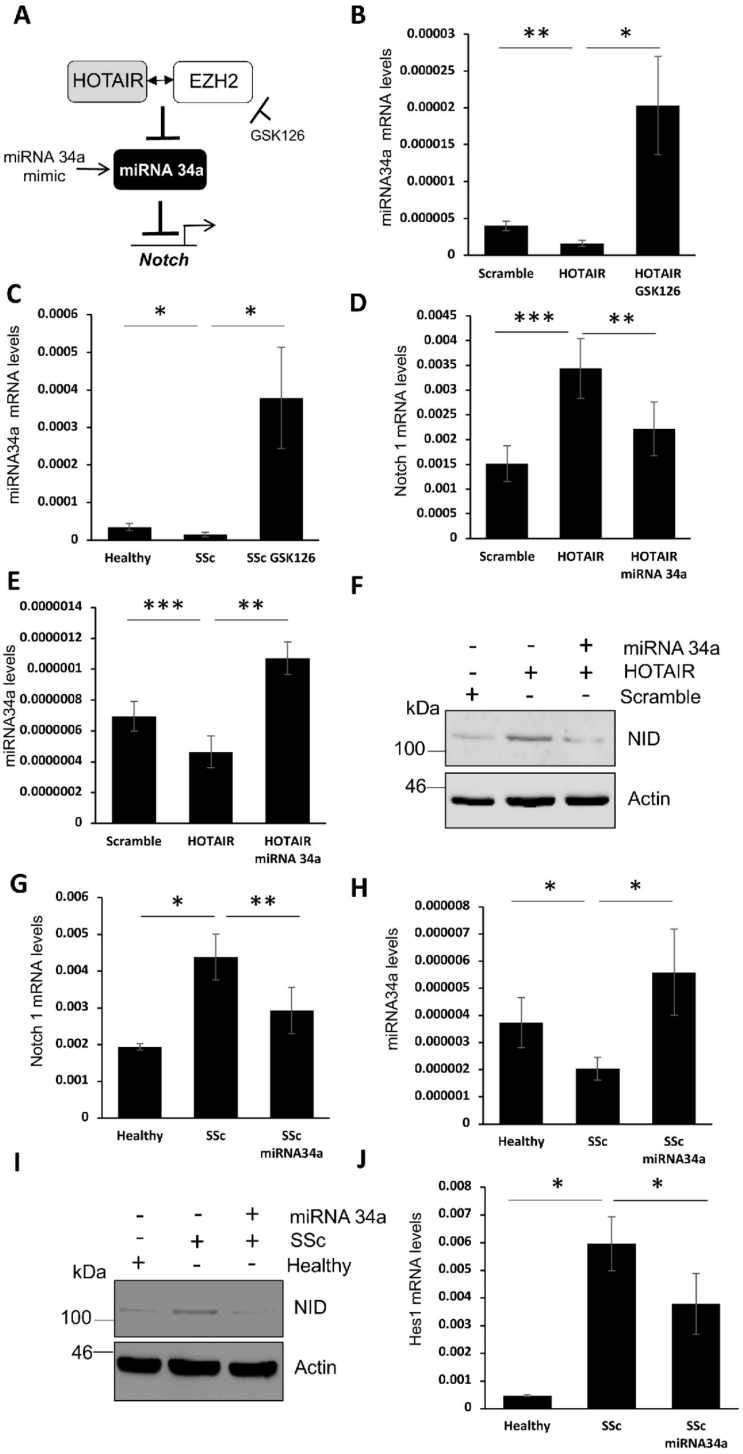

Figure 5 HOX transcript antisense RNA (HOTAIR) drives Notch 1 expression through the methylation of miRNA-34a. (A) Schematic of the mechanism HOTAIR employs to drive Notch transcription. (B) RNA was extracted from fibroblasts stably expressing the scramble and HOTAIR vectors, in addition to HOTAIR fibroblasts treated with the enhancer of zeste 2 (EZH2) inhibitor GSK126. MiRNA-34a transcript levels were assessed by qPCR. Graphs represents mRNA levels from three independent repeats. (C) RNA was extracted from healthy and SSc fibroblasts, in addition systemic sclerosis (SSc) fibroblasts treated with the EZH2 inhibitor GSK126. miRNA-34a transcript levels were assessed by qPCR. Graphs represents mRNA levels from three independent repeats. RNA and protein were extracted from scramble or HOTAIR expressing fibroblasts transfected with an miRNA-34a mimic or a negative control mimic. (D) Notch 1 and (E) miRNA-34a transcript levels were assessed by qPCR. Graphs represents mRNA levels from three independent repeats. (F) Protein lysates were probed with an antibody specific for the intracellular domain of Notch 1 (Notch Intracellular Domain (NID)) by western blot. β-actin was probed for as a loading control. RNA and protein were extracted from healthy and SSc fibroblasts transfected with an miRNA-34a mimic or a negative control mimic. Notch 1 (G) and miRNA-34a (H) transcript levels were assessed by qPCR. Graphs represents mRNA levels from three independent repeats. (I) Protein lysates were probed with an antibody specific for the intracellular domain of Notch 1 (NID) by western blot. β-actin was probed for as a loading control. (J) RNA was extracted from healthy and SSc fibroblasts transfected with an miRNA-34a mimic or a negative control mimic. Hes1 transcript levels were assessed by qPCR. Graphs represents mRNA levels from three independent repeats. *p<0.05, **p<0.01, ***p<0.001.

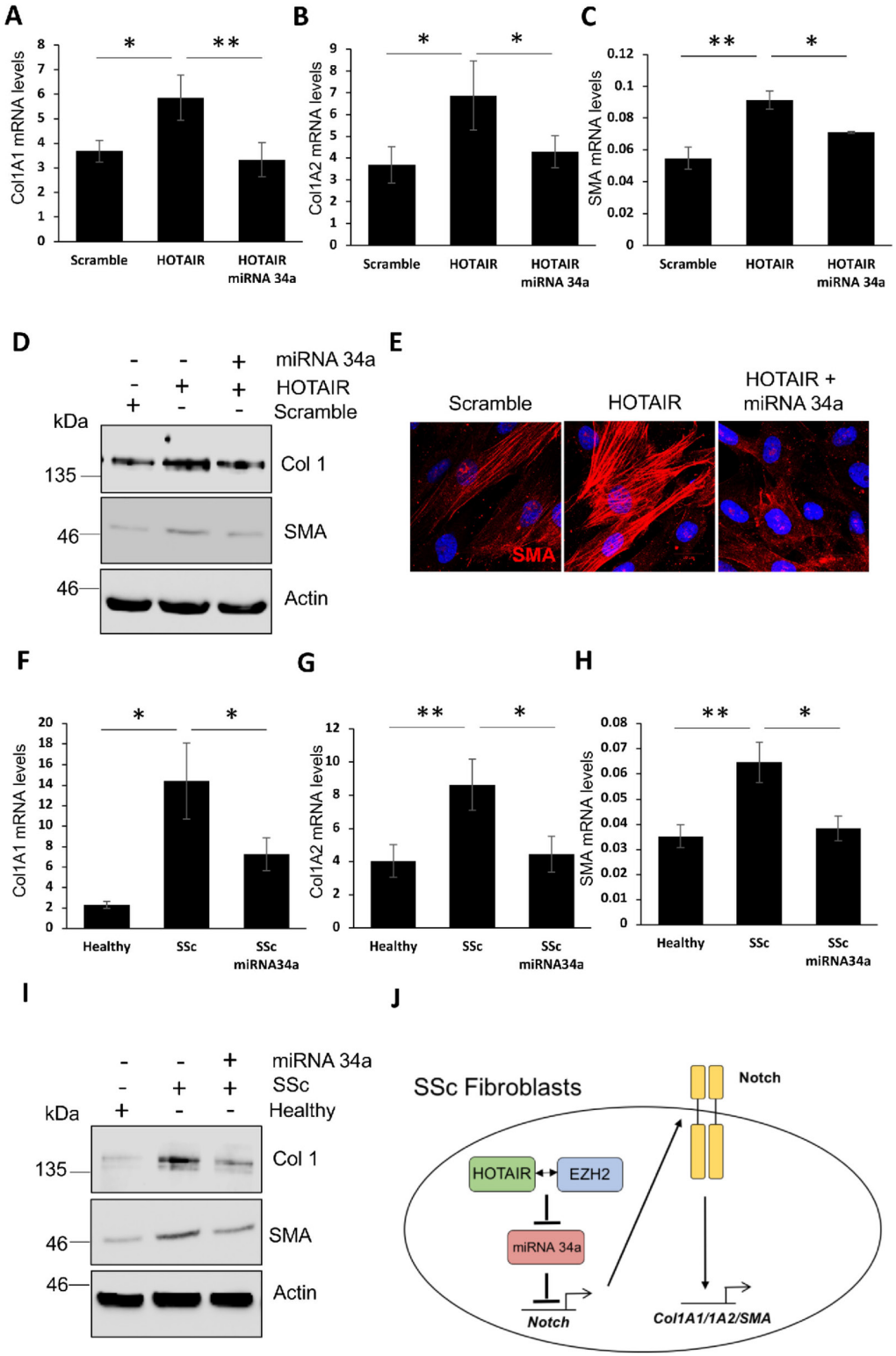

Figure 6 HOX transcript antisense RNA (HOTAIR)-mediated suppression of miRNA-34a is important for systemic sclerosis (SSc) fibrosis. RNA and protein were extracted from scramble or HOTAIR-expressing fibroblasts transfected with an miRNA-34a mimic or a negative control mimic. (A) Col1A1, (B) Col1A2 and (C) alpha-smooth muscle actin (α-SMA) transcript levels were assessed by qPCR. Graphs represents mRNA levels from three independent repeats. (D) Protein lysates were probed with a pan collagen type 1 and α-SMA antibody by western blot. β-actin was probed for as a loading control. (E) α-SMA staining of scramble and HOTAIR expressing dermal fibroblasts, in addition to HOTAIR fibroblasts were transfected with an miRNA-34a mimic or a negative control mimic. Fibroblasts were stained with a mouse α-SMA antibody and visualised with a mouse-specific alexa 594-conjugated secondary (red). Cells were counterstained with DAPI to visualise nuclei (blue). Red lines represent 20 µM scale bar. RNA and protein were extracted from healthy and SSc fibroblasts transfected with an miRNA-34a mimic or a negative control mimic. (F) Col1A1, (G) Col1A2 and (H) α-SMA transcript levels were assessed by qPCR. Graphs represents mRNA levels from three independent repeats. (I) Protein lysates were probed with an collagen type 1 antibody and an α-SMA antibody by western blot. β-actin was probed for as a loading control. (J) Schematic of the role HOTAIR plays in SSc-associated fibrosis. *p<0.05, **p<0.01, ***p<0.001.

Overexpression of miRNA-34a lead to a significant reduction in Col1A1, 1A2 and α-SMA transcript levels (figure 6F–H). This correlated with a reduction in collagen type 1 and α-SMA protein levels when miRNA-34a was overexpressed in SSc fibroblasts (figure 6I).

DISCUSSION

α-SMA expression is a defining marker of myofibroblasts,[41] which are the key cellular elements of tissue fibrosis. The number of myofibroblasts in vivo correlates with severity of disease.[42] It has been well established that fibroblasts cultured from SSc skin biopsies showed increased expression of α-SMA both at RNA and protein levels, which resemble the increased expression of α-SMA induced by TGF-β in dermal fibroblasts derived from HC skin. This observation has supported the studies that have later elucidated the importance of TGF-β in the pathogenesis of tissue fibrosis. When analysed at single-cell level by immunofluorescence, it became apparent that in vitro, the increased expression of α-SMA in SSc fibroblasts, as well as in TGF-β-treated dermal fibroblasts, is due to increased number of α-SMA positive cells (figure 1A) rather than a homogenous increase of α-SMA in all cells. This led us to hypothesise that there is a subpopulation of cells which are epigenetically 'primed' to differentiate into myofibroblasts. Indeed, the most recent single-cell RNA-sequencing analysis of dermal fibroblasts demonstrates the existence of different fibroblast populations in the dermis.[43]

We identified HOTAIR as an epigenetic factor important for the priming of myofibroblasts. Overexpression of HOTAIR in healthy dermal fibroblasts and knockdown of HOTAIR in foreskin fibroblasts modulated expression of α-SMA. A possible limitation of our loss of function studies is that the dermal fibroblasts of these experiments were from a different anatomical location (foreskin). In addition, in vivo studies validating the importance of HOTAIR expression in experimental model of fibrosis will elucidate the importance of this pathway in vivo.

Previous work has shown that SSc fibroblasts extracted from patient skin and cultured for an extended period still have enhanced Notch signalling and this is important for their profibrotic phenotype in vitro and for progression of tissue fibrosis in animal models.[9 10] Evidence presented here shows that HOTAIR is an important epigenetic factor involved in maintaining Notch signalling through enhanced transcription of the receptor. Therefore, HOTAIR may be important for maintaining Notch signalling in SSc fibroblasts in culture. Because of the known HOTAIR function, our data suggested that HOTAIR may play a role in inhibiting gene expression of factors that suppress Notch. The data presented in this study clearly identify miRNA-34a, which is known to suppress Notch1 transcription,[14] as one of the target of HOTAIR-driven gene repression (figure 6J). Nevertheless, it is likely that several other targets are methylated following HOTAIR expression. In addition, it is also possible that miRNA-34a targets a number of other profibrotic targets which requires further investigation.

During this study, Tsou *et al* have shown a critical role of the methyltransferase protein EZH2 in the profibrotic phenotype of SSc fibroblasts. Here, we dissect this phenomenon further by showing that EZH2 methylation profile is driven by HOTAIR and linked to activation of NOTCH. Interestingly, Tsou *et al* found that EZH2 effect on endothelial cells was rescued by NOTCH expression. In this context, our data suggest that EZH2 may play opposite effects in fibroblasts and endothelial cells, which is consistent with fibroblast specific methylation patterns observed in SSc fibroblasts.[44 45]

Beyond NOTCH and TGF-β pathways, other important morphogens have been shown to play a role in the profibrotic phenotype of SSc fibroblasts namely Wnt and sonic hedgehog. Studies elucidating the role of HOTAIR in modulating these pathways would be extremely interesting in future work since we believe they will elucidate the overall role of HOTAIR in tissue homeostasis.

Another recent study identified a novel transcription factor PU.1 as an important regulator of fibrosis. Wohlfahrt *et al* have recently published the importance of PU.1 as transcription factor mediating the TGF-β-induced profibrotic activation in fibroblasts. Nevertheless, in the same study, they have also shown that PU.1 transcription is suppressed by EZH2-dependent methylation.[46] In line with these latter findings, we have observed a reduced expression of PU.1 in our HOTAIR overexpressing fibroblasts (online supplementary figure 3). These data warrant further studies since they suggest that PU.1 and HOTAIR-induced EZH2 methylation may mediate profibrotic activation through distinct or redundant mechanisms. Overall, there is a growing body of evidence to suggest that inhibitors of the PRC2 may represent a viable therapeutic target for SSc.

Our studies explored the effects of HOTAIR upregulation in the fibrosis associated with SSc, but left unanswered the question on how HOTAIR is upregulated in SSc. There is evidence to suggest that Rho GTPase/ROCK signalling is important for HOTAIR expression in breast cancer.[47] Inhibition of ROCK lead to a reduction in HOTAIR transcript levels. Rho GTPases may enhance HOTAIR transcription in SSc fibroblasts. Since it is well established that inhibition of Rho GTPase and ROCK in scleroderma fibroblasts leads to a reduction collagen production and SMA expression,[48] it is possible that Rho GTPase may drive SSc fibrosis through enhanced HOTAIR expression. In our opinion, this is an interesting hypothesis which deserves further investigation.

Overall, our data show that HOTAIR is overexpressed in SSc fibroblasts and this overexpression is important for myofibroblast activation through EZH2/PRC2 H3K27me3 methylation. In addition, our data may offer a potential explanation of why skin fibrosis in patients with SSc starts in the hands and feet which are regions with a physiologically higher expression of HOTAIR in dermal fibroblasts.[25]

Author affiliations
[1]Leeds Institute of Rheumatic and Musculoskeletal Medicine, University of Leeds, Leeds, UK
[2]Rheumatology Department of Lucania San Carlo Hospital, Potenza, Italy, Rheumatology Institute of Lucania (IReL), Potenza, Italy
[3]Scleroderma Programme, NIHR Leeds Musculoskeletal Biomedical Research Centre, Leeds, UK
[4]Jefferson Institute of Molecular Medicine, Thomas Jefferson University, Philadelphia, Pennsylvania, USA
[5]Rheumatology, Medical University of South Carolina, Charlestown, South Carolina, USA
[6]Center for Personal Dynamic Regulomes, University of Stanford, San Francisco, California, USA

Twitter Francesco del Galdo @delgaldoFrances

Contributors CWW performed most of the experiments and wrote the manuscript with FdG. HH and FdG performed the LCM experiments. GA, MM and RLR performed some of the gene expression experiments. CWW, FdG and CAF-B designed the experimental plan. FdG, CAF-B and SAJ conceived the study. HC generated LncRNA tiling array data and contributed to manuscript draft.

Competing interests H.Y.C. is a co-founder of Accent Therapeutics, Boundless Bio, and advisor to 10x Genomics, Arsenal Biosciences, and Spring Discovery.

Patient consent for publication Not required.

Provenance and peer review Not commissioned; externally peer reviewed.

Data availability statement Data are available upon reasonable request. All data relevant to the study are included in the article or uploaded as supplementary information. All raw data are available upon request.

ORCID iDs
Sergio A Jimenez http://orcid.org/0000-0001-5213-1203
Francesco del Galdo http://orcid.org/0000-0002-8528-2283

REFERENCES

1 Gabrielli A, Avvedimento EV, Krieg T. Scleroderma. *N Engl J Med* 2009;360:1989–2003.
2 Denton CP, Khanna D. Systemic sclerosis. *Lancet* 2017;390:1685–99.
3 Lambova S, Batalov A, Dobrev H, *et al*. Digital Ulcers in Systemic Sclerosis - How to Manage in 2013? *Curr Rheumatol Rev* 2013;9:274–8.
4 Garrett SM, Baker Frost D, Feghali-Bostwick C. The mighty fibroblast and its utility in scleroderma research. J scleroderma relat Disord. *May-Aug* 2017;2:69–134.
5 Hinz B, Phan SH, Thannickal VJ, *et al*. Recent developments in myofibroblast biology: paradigms for connective tissue remodeling. *Am J Pathol* 2012;180:1340–55.
6 Kawakami T, Ihn H, Xu W, *et al*. Increased expression of TGF-beta receptors by scleroderma fibroblasts: evidence for contribution of autocrine TGF-beta signaling to scleroderma phenotype. *J Invest Dermatol* 1998;110:47–51.
7 Varga J, Pasche B. Transforming growth factor beta as a therapeutic target in systemic sclerosis. *Nat Rev Rheumatol* 2009;5:200–6.
8 Zehender A, Huang J, Györfi A-H, *et al*. The tyrosine phosphatase SHP2 controls TGFβ-induced STAT3 signaling to regulate fibroblast activation and fibrosis. *Nat Commun* 2018;9:3259.
9 Iwayama T, Olson LE. Involvement of PDGF in fibrosis and scleroderma: recent insights from animal models and potential therapeutic opportunities. *Curr Rheumatol Rep* 2013;15:304.
10 Liakouli V, Elies J, El-Sherbiny YM, *et al*. Scleroderma fibroblasts suppress angiogenesis via TGF-β/caveolin-1 dependent secretion of pigment epithelium-derived factor. *Ann Rheum Dis* 2018;77:431–40.
11 Dees C, Tomcik M, Zerr P, *et al*. Notch signalling regulates fibroblast activation and collagen release in systemic sclerosis. *Ann Rheum Dis* 2011;70:1304–10.
12 Dees C, Zerr P, Tomcik M, *et al*. Inhibition of Notch signaling prevents experimental fibrosis and induces regression of established fibrosis. *Arthritis Rheum* 2011;63:1396–404.
13 Hori K, Sen A, Artavanis-Tsakonas S. Notch signaling at a glance. *J Cell Sci* 2013;126:2135–40.
14 Andersson ER, Sandberg R, Lendahl U. Notch signaling: simplicity in design, versatility in function. *Development* 2011;138:3593–612.
15 Guruharsha KG, Kankel MW, Artavanis-Tsakonas S. The Notch signalling system: recent insights into the complexity of a conserved pathway. *Nat Rev Genet* 2012;13:654–66.
16 Kwon H, Song K, Han C, *et al*. Epigenetic silencing of miRNA-34a in human cholangiocarcinoma via EZH2 and DNA methylation: impact on regulation of Notch pathway. *Am J Pathol* 2017;187:2288–99.
17 Di Bari M, Bevilacqua V, De Jaco A, *et al*. Mir-34a-5p mediates cross-talk between M2 muscarinic receptors and Notch-1/EGFR pathways in U87MG glioblastoma cells: implication in cell proliferation. *Int J Mol Sci* 2018;19. doi:10.3390/ijms19061631. [Epub ahead of print: 31 May 2018].
18 Tsou P-S, Campbell P, Amin MA, *et al*. Inhibition of EZH2 prevents fibrosis and restores normal angiogenesis in scleroderma. *Proc Natl Acad Sci U S A* 2019;116:3695–702.
19 Novikova IV, Hennelly SP, Sanbonmatsu KY. Sizing up long non-coding RNAs: do lncRNAs have secondary and tertiary structure? *Bioarchitecture* 2012;2:189–99.
20 Brockdorff N, Noncoding RNA. And polycomb recruitment. *RNA* 2013;19:429–42.
21 Yoon J-H, Abdelmohsen K, Kim J, *et al*. Scaffold function of long non-coding RNA HOTAIR in protein ubiquitination. *Nat Commun* 2013;4:2939.
22 Peng H, Wan L-Y, Liang J-J, *et al*. The roles of lncRNA in hepatic fibrosis. *Cell Biosci* 2018;8:63.
23 Micheletti R, Plaisance I, Abraham BJ, *et al*. The long noncoding RNA *Wisper* controls cardiac fibrosis and remodeling. *Sci Transl Med* 2017;9. doi:10.1126/scitranslmed.aai9118
24 Sun SF, Tang PMK, Feng M, *et al*. Novel lncRNA Erbb4-IR Promotes Diabetic Kidney Injury in *db/db* Mice by Targeting miR-29b. *Diabetes* 2018;67:731–44.
25 Rinn JL, Kertesz M, Wang JK, *et al*. Functional demarcation of active and silent chromatin domains in human Hox loci by noncoding RNAs. *Cell* 2007;129:1311–23.
26 Gupta RA, Shah N, Wang KC, *et al*. Long non-coding RNA HOTAIR reprograms chromatin state to promote cancer metastasis. *Nature* 2010;464:1071–6.
27 Kogo R, Shimamura T, Mimori K, *et al*. Long noncoding RNA HOTAIR regulates polycomb-dependent chromatin modification and is associated with poor prognosis in colorectal cancers. *Cancer Res* 2011;71:6320–6.
28 Wu L, Murat P, Matak-Vinkovic D, *et al*. Binding interactions between long noncoding RNA HOTAIR and PRC2 proteins. *Biochemistry* 2013;52:9519–27.
29 Fuzii HT, Yoshikawa GT, Junta CM, *et al*. Affected and non-affected skin fibroblasts from systemic sclerosis patients share a gene expression profile deviated from the one observed in healthy individuals. *Clin Exp Rheumatol* 2008;26:866–74.
30 Zhu L, Gao D, Yang J, *et al*. Characterization of the phenotype of high collagen-producing fibroblast clones in systemic sclerosis, using a new modified limiting-dilution method. *Clin Exp Dermatol* 2012;37:395–403.
31 Tsai M-C, Manor O, Wan Y, *et al*. Long noncoding RNA as modular scaffold of histone modification complexes. *Science* 2010;329:689–93.
32 Kaneko S, Li G, Son J, *et al*. Phosphorylation of the PRC2 component EZH2 is cell cycle-regulated and up-regulates its binding to ncRNA. *Genes Dev* 2010;24:2615–20.
33 McCabe MT, Ott HM, Ganji G, *et al*. Ezh2 inhibition as a therapeutic strategy for lymphoma with EZH2-activating mutations. *Nature* 2012;492:108–12.
34 Kim J-E, Lee J-H, Jeong K-H, *et al*. Notch intracellular domain expression in various skin fibroproliferative diseases. *Ann Dermatol* 2014;26:332–7.
35 Lee M, Kim HJ, Kim SW, *et al*. The long non-coding RNA HOTAIR increases tumour growth and invasion in cervical cancer by targeting the Notch pathway. *Oncotarget* 2016;7:44558–71.
36 Dong C, Liu S, Lv Y, *et al*. Long non-coding RNA *HOTAIR* regulates proliferation and invasion via activating Notch signalling pathway in retinoblastoma. *J Biosci* 2016;41:677–87.
37 Zhao W, Dong L. Long non-coding RNA HOTAIR overexpression improves premature ovarian failure by upregulating Notch-1 expression. *Exp Ther Med* 2018;16:4791–5.
38 Gonzalez ME, Moore HM, Li X, *et al*. Ezh2 expands breast stem cells through activation of Notch1 signaling. *Proc Natl Acad Sci U S A* 2014;111:3098–103.
39 Lee SM, Moon J, Redman BG, *et al*. Phase 2 study of ro4929097, a gamma-secretase inhibitor, in metastatic melanoma: SWOG 0933. *Cancer* 2015;121:432–40.
40 Geling A, Steiner H, Willem M, *et al*. A gamma-secretase inhibitor blocks Notch signaling in vivo and causes a severe neurogenic phenotype in zebrafish. *EMBO Rep* 2002;3:688–94.
41 Gilbane AJ, Denton CP, Holmes AM. Scleroderma pathogenesis: a pivotal role for fibroblasts as effector cells. *Arthritis Res Ther* 2013;15:215.
42 Farina G, Lemaire R, Pancari P, *et al*. Cartilage oligomeric matrix protein expression in systemic sclerosis reveals heterogeneity of dermal fibroblast responses to transforming growth factor beta. *Ann Rheum Dis* 2009;68:435–41.
43 Philippeos C, Telerman SB, Oulès B, *et al*. Spatial and single-cell transcriptional profiling identifies functionally distinct human dermal fibroblast subpopulations. *J Invest Dermatol* 2018;138:811–25.
44 Altorok N, Almeshal N, Wang Y, *et al*. Epigenetics, the Holy Grail in the pathogenesis of systemic sclerosis. rheumatology (Oxford). 2015;54:1759–70.
45 Altorok N, Tsou P-S, Coit P, *et al*. Genome-Wide DNA methylation analysis in dermal fibroblasts from patients with diffuse and limited systemic sclerosis reveals common and subset-specific DNA methylation aberrancies. *Ann Rheum Dis* 2015;74:1612–20.
46 Wohlfahrt T, Rauber S, Uebe S, *et al*. Pu.1 controls fibroblast polarization and tissue fibrosis. *Nature* 2019;566:344–9.
47 He H, Wei Z, Du F, *et al*. Transcription of HOTAIR is regulated by RhoC-MRTF-A-SRF signaling pathway in human breast cancer cells. *Cell Signal* 2017;31:87–95.
48 Akhmetshina A, Dees C, Pileckyte M, *et al*. Rho-Associated kinases are crucial for myofibroblast differentiation and production of extracellular matrix in scleroderma fibroblasts. *Arthritis Rheum* 2008;58:2553–64.